STRUCTURAL
BIOLOGY

Volume 78 (2022)

Supporting information for article:

Unravelling the regulation pathway of photosynthetic AB-GAPDH

Roberto Marotta, Alessandra Del Giudice, Libero Gurrieri, Silvia Fanti, Paolo Swuec, Luciano Galantini, Giuseppe Falini, Paolo Trost, Simona Fermani and Francesca Sparla

Table S1 Summary of SAXS data acquisition information, sample details, and data analysis software used.

(A) Sample details for the SEC-SAXS experiments			
	inhibited	active-short	active
Loading concentration (mg ml^{-1})	13	11	< 5
Injection volume (µl)	100	200	200
Storage buffer composition	25 mM K-phosphate, pH 7.5, 0.1 mM NAD^+	25 mM K-phosphate, pH 7.5, 5 mM reduced DTT, 20 mM $NADP^+$ 1,3-bisphosphoglycerate*	25 mM K-phosphate, pH 7.5, 5 mM reduced DTT, 20 mM $NADP^+$ 1,3-bisphosphoglycerate*
Elution buffer composition	25 mM K-phosphate, pH 7.5, 0.1 mM NAD^+	25 mM K-phosphate, pH 7.5, 0.1 mM $NADP^+$	25 mM K-phosphate, pH 7.5, 0.1 mM $NADP^+$

*obtained by incubation of phosphoglycerate kinase, 20 U ml^{-1}, with 15 mM 3-phosphoglyceric acid, 10 mM ATP and 5 mM MgCl2

(B) SAXS data collection parameters for the SEC-SAXS experiments	
Source, instrument	ESRF, BM29 (Pernot et al., 2013)
Wavelength (Å)	0.9919
Sample-to-detector distance (m)	2.872
$q=4\pi\sin(\theta)/\lambda$ (2θ scattering angle) range (Å^{-1})	0.005-0.45
Absolute scaling method	water scattering I(0)= 0.01632 cm^{-1}, protein partial specific volume 0.735 cm^3 g^{-1}
Exposure time (s)	1
Capillary path length (mm)	1.8
SEC column	Superdex 200 10/300 GL (GE Healthcare)
Flow rate (ml·min^{-1})	0.5
SEC column temperature (ºC)	22

(C) Sample details for the SC-SAXS experiments		
	inhibited	active
Concentration range (mg ml^{-1})	0.08-1.89	0.1-2.0
Storage and dilution buffer composition	25 mM K-phosphate, pH 7.5, 1 mM NAD^+	25 mM K-phosphate, pH 7.9, 1 mM $NADP^+$

(D) SAXS data collection parameters for the SC-SAXS experiments		
	inhibited	active
Source, instrument	ESRF, BM29 (Pernot et al., 2013)	
Wavelength (Å)	0.9919	
sample-to-detector distance (m)	2.872	2.864
q-measurement range ($Å^{-1}$)	0.005-0.45	
Absolute scaling method	water scattering I(0)= 0.01632 cm^{-1}, protein partial specific volume 0.735 cm^3 g^{-1}	
Capillary path length (mm)	1.8	
Injection volume (µl)	50	60
Exposure time (s)	1	2
Number of exposures	10	10
Extra flow time (s)	10	10
Sample temperature (ºC)	4	5

(E) Software employed for SAS data reduction, analysis, and interpretation	
Solvent subtraction, averaging and basic analysis (Guinier fit, P(r), Porod Volume)	Matlab scripts, ATSAS 2.8 (Franke et al., 2017)
Theoretical intensity calculations	CRYSOL 3.0, OLIGOMER
Molecular graphics	PyMOL 1.8

Table S2 CryoEM data collection and data processing parameters.

DATA COLLECTION	
Microscope model	Thermo Fisher Scientific Tecnai Polara F30
Detector type	GATAN K2 Summit
Imaging mode	Bright field
Accelerating voltage, kV	300
Nominal/Calibrated magnification	31000
Pixel size, Å	1.21
Total exposure time, sec	4
Total Number of collected stacks	2228
Number of stacks used in the analysis	1988
Total dose per stack, $e^{-}/Å^2$	42
Number of frames per stack	40
Defocus range, μm	from -1.5 to -3.5
Defocus step, μm	0.15

DATA PROCESSING, GLOBAL RESOLUTION (Å) AND EMDB ID	
3D reconstruction software package	Relion 3.0
A2B2	
Extracted particles	48558
Refined particles	19636
Symmetry	D2
FSC0.143 (unmasked/masked)	6.5/6.3
Local resolution range, Å	3.7-9.7
EMBD ID	13824
A4B4	
Extracted particles	31023
Refined particles	20777
Symmetry	C1
FSC0.143 (unmasked/masked)	13.1/8.9
Local resolution range, Å	4-15
EMBD ID	13825
A8B8 main conformer	
Extracted particles	64130
Refined particles	23611
Symmetry	C2
FSC0.143 (unmasked/masked)	7.4/5.7
Local resolution range, Å	3.7-10.2
EMBD ID	13826

A8B8 alternative conformer	
Extracted particles	64130
Refined particles	10768
Symmetry	C2
FSC0.143 (unmasked/masked)	8.2/7.1
Local resolution range, Å	4-11.5
EMBD ID	13827
A10B10	
Total extracted particles	33067
Refined particles	7352
Symmetry	C5
FSC0.143 (unmasked/masked)	15.1/13
Local resolution range, Å	4.7-14.7
EMBD ID	13828

Table S3 Detailed summary of the SEC-SAXS data analysis of AB-GAPDH samples.

	inhibited			active-short			active
SAXS frame at injection	90			222			268
Background data							
frames	1-1295			1-1650			1-1886
max VSEC (ml)	10			11.9			13.5
Selected protein data							
frames	1510-1540	1638-1728	1860-1900	1840-1860	1972-2027	2170-2193	2090-2140
VSEC interval (ml)	11.8-12.1	12.9-13.7	14.8-15.1	13.5-13.7	14.6-15.0	16.2-16-4	15.2-15.6
<VSEC> (ml)	12.0	13.3	14.9	13.6	14.8	16.3	15.4
Guinier fit							
Rg (Å)	80.6	66.8	59.6	50.9	39.4	34.0	33.9
σ(Rg) (Å)	1.0	0.1	1.5	0.6	0.1	0.4	0.1
I(0) [kDa c(mg ml^{-1})]	117.9	248.5	16.0	27.2	125.8	23.3	34.0
σ(I(0))	0.5	0.2	0.3	0.3	0.1	0.2	0.1
First q point (Å^{-1})	0.007	0.007	0.013	0.130	0.120	0.220	0.016
Last q point (Å^{-1})	0.016	0.019	0.022	0.025	0.029	0.038	0.038
Auto Rg quality	0.89	0.87	0.96	0.74	0.97	0.99	0.96
Indirect Fourier transform							
Rg (Å)	82.7	66.9	67.2	53.2	40.3	33.9	34.1
σ(Rg) (Å)	0.4	0.1	3.3	0.6	0.1	0.3	0.1
I(0) [kDa c(mg ml^{-1})]	119.3	248.7	16.7	27.6	126.4	23.2	34.2
σ(I(0))	0.4	0.2	0.5	0.2	0.1	0.1	0.1
VP (10^{-3} Å^3)	1100	830	508	346	228	183	201
First q point (Å^{-1})	0.007	0.007	0.013	0.013	0.012	0.022	0.016
Last q point (Å^{-1})	0.25	0.25	0.25	0.25	0.25	0.25	0.25
Dmax imposed for P(r) (Å)	276	217	280	180	146	112	112
Dmax variability estimate (Å)	15	10	25	10	10	5	5
GNOM quality estimate	0.74	0.74	0.65	0.73	0.63	0.75	0.75
MW(VP)[a] (kDa)	647	488	299	203	134	107	118
MW (Vc)[b] (kDa)	712	555	222	208	147	112	132
MW (MoW)[c] (kDa)	681	568	231	225	173	122	148
MW Bayesian[d]							
estimate (kDa)	715	479	318	243	147	119	147
estimate probability (%)	94.6	95.0	79.1	89.0	48.8	46.5	50.4

credibility interval (kDa)	614-751	455-556	221-373	195-264	142-177	111-127	127-151
interval probability (%)	99.8	98.4	99.8	99.6	98.0	92.7	95.9

[a]From the Porod volume VP according to the empirical relation MW~0.625 VP (Petoukhov et al., 2012); [b]From the volume of correlation Vc (qmax for integration 0.25 $Å^{-1}$) (Rambo & Tainer, 2013); [c]From the Porod invariant (qmax for integration 0.25 $Å^{-1}$) (Fisher et al., 2010); [d]From the Bayesian inference approach based on concentration-independent methods (Hajizadeh et al., 2018).

Table S4 Summary of dimensional parameters obtained by the analysis of selected SAXS profiles collected during the SEC elution of AB-GAPDH samples.

		Guinier	P(r)		Porod volume	MW estimate		Possible stoichiometry	
Sample	<VSEC > (ml)	Rg (Å)	Rg (Å)	Dmax (Å)[a]	(10^{-3} Å^3)	MW[b]	MW[c]	MW (kDa)	
inhibited									
	12.0	80.6 ± 1.0	82.7 ± 0.4	270 ± 20	1100	834	715 ± 24	A10B10	741
	13.3	66.8 ± 0.1	66.9 ± 0.1	200 ± 10	830	504	479 ± 20	A8B8	607
	14.9	59.6 ± 1.5	67.2 ± 3.3	180 ± 30	508	266	318 ± 27	A4B4	299
active-short									
	13.6	50.9 ± 0.6	53.2 ± 0.6	170 ± 10	346	208	243 ± 13	A4B4	299
	14.8	39.4 ± 0.1	40.3 ± 0.1	140 ± 20	228	153	147 ± 9	A2B2	149
	16.3	34.0 ± 0.4	33.9 ± 0.3	110 ± 10	183	118	119 ± 6	A2B2	149
active									
	15.4	33.9 ± 0.1	34.1 ± 0.1	100 ± 10	201	134	147 ± 7	A2B2	149

[a]Estimated from the distance value at which the P(r) function calculated from indirect Fourier transform approaches zero; [b]From the Porod volume VP according to the empirical relation MW~0.625 VP (Petoukhov et al., 2012); [c]From the Bayesian inference approach based on concentration-independent methods (Hajizadeh et al., 2018).

Table S5 Cross correlation values for A-subunit or B-subunit positioned in the contact region between adjacent tetramers in the various GAPDH oligomers. The values have been calculated using the "fit" command as implemented in UCSF Chimera (Afonine *et al.*, 2018).

	GAPDH oligomer							
	A4B4		A8B8 Main conf.		A8B8 Alt. Conf.		A10B10	
	A-sub.	B-sub.	A-sub.	B-sub.	A-sub.	B-sub.	A-sub.	B-sub
	0.9416	0.9464	0.9270	0.9334	0.9434	0.9493	0.9744	0.9759
	0.9408	0.9462	0.9270	0.9334	0.9431	0.9493	0.9744	0.9759
	0.9405	0.9449	0.9268	0.9334	0.9411	0.9487	0.9743	0.9758
	0.9397	0.9447	0.9268	0.9326	0.9411	0.9487	0.9743	0.9758
			0.9261	0.9325	0.9406	0.9464	0.9743	0.9758
			0.9260		0.9406	0.9461	0.9743	0.9758
						0.9461	0.9743	0.9758
								0.9758
Average	0.9410	0.9460	0.9270	0.9330	0.9420	0.9480	0.9740	0.9760
SD	0.0008	0.0009	0.0004	0.0005	0.0013	0.0015	0.00005	0.00005
t-test	0.000170926		$5.5205 \cdot 10^{-9}$		$6.80329 \cdot 10^{-6}$		$7.6780 \cdot 10^{-17}$	

Table S6 GAPDH oligomers average interface areas and ΔG calculated by PDBePISA (Krissinel & Henrick, 2007).

GAPDH oligomer	**N° Interfaces**	**Total Interface Area**	**Single Interface Area**	**ΔGint**	**ΔGdiss**
	(#)	(Å^2)		(kcal mol^{-1})	
A4B4	1	656	656	-234.6	35.9
A4B4 (no CTE)	1	403	403	-212.4	-12.4
A8B8 Main Conf.	4	2641	660	-537.9	41.0
A8B8 Main Conf. (no CTE)	4	1795	449	-484.0	-17.0
A8B8 Alt. Conf.	4	2501	625	-732.7	35.5
A8B8 Alt. Conf. (no CTE)	4	1684	421	-668.6	-17.0
A10B10	5	1139	228	-618.6	-34.7

Table S7 Results of the optimization of the selected averaged SAXS profiles in the SEC-SAXS experiments as a linear combination of AB-GAPDH oligomers. The χ^2 value obtained by fitting the data with a single structural model are reported in the last column for comparison.

			Optimized volume fractions				Calculated			
Sample	<VSEC> (ml)	AB (OR)	A2B2[a]	A4B4	A8B8[b]	A10B10	MW (kDa)	Rg (Å)	χ^2	χ^{2c}
inhibited										
	12.0	-	0	0.154 ± 0.005	0.057 ± 0.008	0.789 ± 0.006	687	77.1	2.4	4.9
	13.3	-	0	0.131 ± 0.001	0.753 ± 0.042	0.116 ± 0.002	591	66.8	4.9	19.2
	14.9	-	0.079 ± 0.176	0.719 ± 0.242	0.162 ± 0.113	0.040 ± 0.035	357	57.8	1.0	1.0
active-short										
	13.6	0	0.114 ± 0.053	0.849 ± 0.069	0.037 ± 0.023	0	294	51.5	1.0	1.0
	14.8	0.146 ± 0.002	0.570 ± 0.002	0.284 ± 0.001	0	0	181	42.2	10.1	143
	16.3	0.332 ± 0.015	0.650 ± 0.013	0.018 ± 0.006	0	0	128	33.0	0.9	1.4
active										
	15.4	0.101 ± 0.007	0.854 ± 0.006	0.045 ± 0.003	0	0	149	34.6	1.1	2.1

[a]From the A2B2 crystal structure (PDB ID 2PKQ) (Fermani et al., 2007); [b]Both the cryoEM derived models of A8B8 were included (main population and alternative conformation) and here the sum of their volume fractions is reported. Their theoretical scattering profile is almost indistinguishable, as seen in Fig. S9; [c]By fitting the selected data with the theoretical scattering profile of a single structural model with CRYSOL 3.0 in fitting mode, as explained in the caption of Fig. S10.

Table S8 Summary of the SC-SAXS data analysis.

Sample	**inhibited**							
Concentration (mg ml^{-1})	1.89	1.52	1.18	0.67	0.52	0.39	0.2	0.08
Guinier fit								
Rg (Å)	82.2	84.6	82.0	81.0	80.8	81.1	80.8	88.9
σ(Rg) (Å)	3.4	4.5	8.7	17.5	20.6	60.0	16.9	11.6
I(0) [kDa]	530	546	513	561	509	490	470	509
σ(I(0))	2	1	1	3	3	4	4	9
First q point (Å^{-1})	0.0075	0.0075	0.0089	0.0099	0.0100	0.0108	0.0080	0.0075
Last q point (Å^{-1})	0.015	0.012	0.015	0.016	0.016	0.016	0.016	0.015
AutoRg quality	0.85	0.78	0.78	0.74	0.71	0.41	0.56	0.42
Indirect Fourier transform								
Rg (Å)	86.0	85.6	86.9	88.2	86.9	88.6	85.6	93.7
σ(Rg) (Å)	0.2	0.3	0.4	0.5	0.8	1.3	1.7	2.3
I(0) [kDa]	536.0	543.5	521.6	581.7	525.1	510.9	477.1	511.6
σ(I(0))	0.9	1.0	1.6	2.3	2.9	4.6	5.7	10.7
VP (10^{-3} Å^3)	1240	1220	1260	1310	1270	1370	1210	1460
First q point (Å^{-1})	0.0075	0.0075	0.0089	0.0099	0.0100	0.0108	0.0800	0.0750
Last q point (Å^{-1})	0.35	0.35	0.35	0.35	0.35	0.35	0.35	0.35
Dmax imposed for P(r) (Å)	340	340	340	340	340	340	340	340
Dmax variability estimate (Å)	50	50	50	50	50	50	50	50
GNOM quality estimate	0.53	0.53	0.53	0.54	0.50	0.52	0.55	0.46
MW(VP)[a] (kDa)	775	763	788	819	794	856	756	913
MW (Vc)[b] (kDa)	626	627	625	619	608	658	607	573
MW (MoW)[c] (kDa)	661	663	658	625	589	687	580	466
Sample	**active**							
Concentration (mg ml^{-1})	2	1	0.5	0.25	0.1			
Guinier fit								
Rg (Å)	66.5	63.0	60.5	54.5	50.2			
σ(Rg) (Å)	1.5	1.0	2.9	2.8	1.5			
I(0) [kDa]	134.1	111.6	95.0	76.5	63.7			
σ(I(0))	0.2	0.2	0.3	0.3	0.7			
First q point (Å^{-1})	0.0097	0.0055	0.0060	0.0060	0.0070			

Last q point (Å^{-1})	0.0187	0.0192	0.0187	0.0234	0.0258
AutoRg quality	0.75	0.64	0.82	0.45	0.26
Indirect Fourier transform					
Rg (Å)	70.5	66.6	63.7	59.7	53.9
σ(Rg) (Å)	0.3	0.4	0.6	1.1	2.1
I(0) [kDa]	137.0	113.0	95.8	78.2	64.4
σ(I(0))	0.3	0.2	0.4	0.6	1.1
VP (10-3 Å^3)	502	431	363	329	258
First q point (Å^{-1})	0.0097	0.0055	0.0060	0.0060	0.0070
Last q point (Å^{-1})	0.35	0.35	0.35	0.35	0.35
Dmax imposed for P(r) (Å)	300	280	250	240	230
Dmax variability estimate (Å)	100	20	50	30	30
GNOM quality estimate	0.48	0.52	0.46	0.47	0.42
MW(VP)[a] (kDa)	314	270	227	206	161
MW (Vc)[b] (kDa)	312	253	185	168	139
MW (MoW)[c] (kDa)	377	329	219	217	179

[a]From the Porod volume VP according to the empirical relation MW~0.625 VP (Petoukhov et al., 2012); [b]From the volume of correlation Vc (qmax for integration 0.25 Å^{-1}) (Rambo & Tainer, 2013); [c]From the Porod invariant (qmax for integration 0.25 Å^{-1}) (Fisher et al., 2010).

Table S9 Results of the optimization of the SC-SAXS data for concentration series of active and inhibited AB-GAPDH samples as a linear combination of AB-GAPDH oligomers.

		Optimized volume fractions					Calculated	
Sample	(mg ml^{-1})	A2B2	A4B4	A8B8[a]	A10B10	χ^2	MW (kDa)	Rg (Å)
inhibited	1.89	0	0.163 ± 0.001	0.377 ± 0.002	0.460 ± 0.002	19.1	634	72.6
	1.52	0	0.160 ± 0.002	0.377 ± 0.003	0.463 ± 0.002	13.1	635	72.6
	1.18	0	0.162 ± 0.002	0.362 ± 0.003	0.476 ± 0.003	8.8	636	72.9
	0.67	0	0.161 ± 0.003	0.334 ± 0.005	0.504 ± 0.004	4.8	641	73.3
	0.52	0	0.157 ± 0.004	0.329 ± 0.006	0.513 ± 0.005	3.3	644	73.4
	0.39	0	0.147 ± 0.005	0.307 ± 0.008	0.545 ± 0.007	2.0	652	73.9
	0.20	0	0.146 ± 0.009	0.372 ± 0.016	0.482 ± 0.012	1.0	643	73.0
	0.08	0	0.128 ± 0.023	0.355 ± 0.037	0.517 ± 0.028	0.8	653	73.5
active								
	2.00	0.181 ± 0.011	0.507 ± 0.017	0.042 ± 0.009	0.270 ± 0.003	11.4	412	66.8
	1.00	0.335 ± 0.021	0.445 ± 0.031	0.022 ± 0.016	0.197 ± 0.005	2.2	350	63.5
	0.50	0.453 ± 0.008	0.395 ± 0.009	0	0.152 ± 0.003	1.7	305	60.5
	0.25	0.551 ± 0.016	0.336 ± 0.019	0	0.113 ± 0.005	0.8	272	57.3
	0.10	0.643 ± 0.041	0.283 ± 0.046	0	0.074 ± 0.013	0.8	240	53.1

[a]Both the cryoEM derived models of A8B8 were included (main population and alternative conformation) and here the sum of their volume fractions is reported. Their theoretical scattering profile is almost indistinguishable, as seen in Fig. S9.

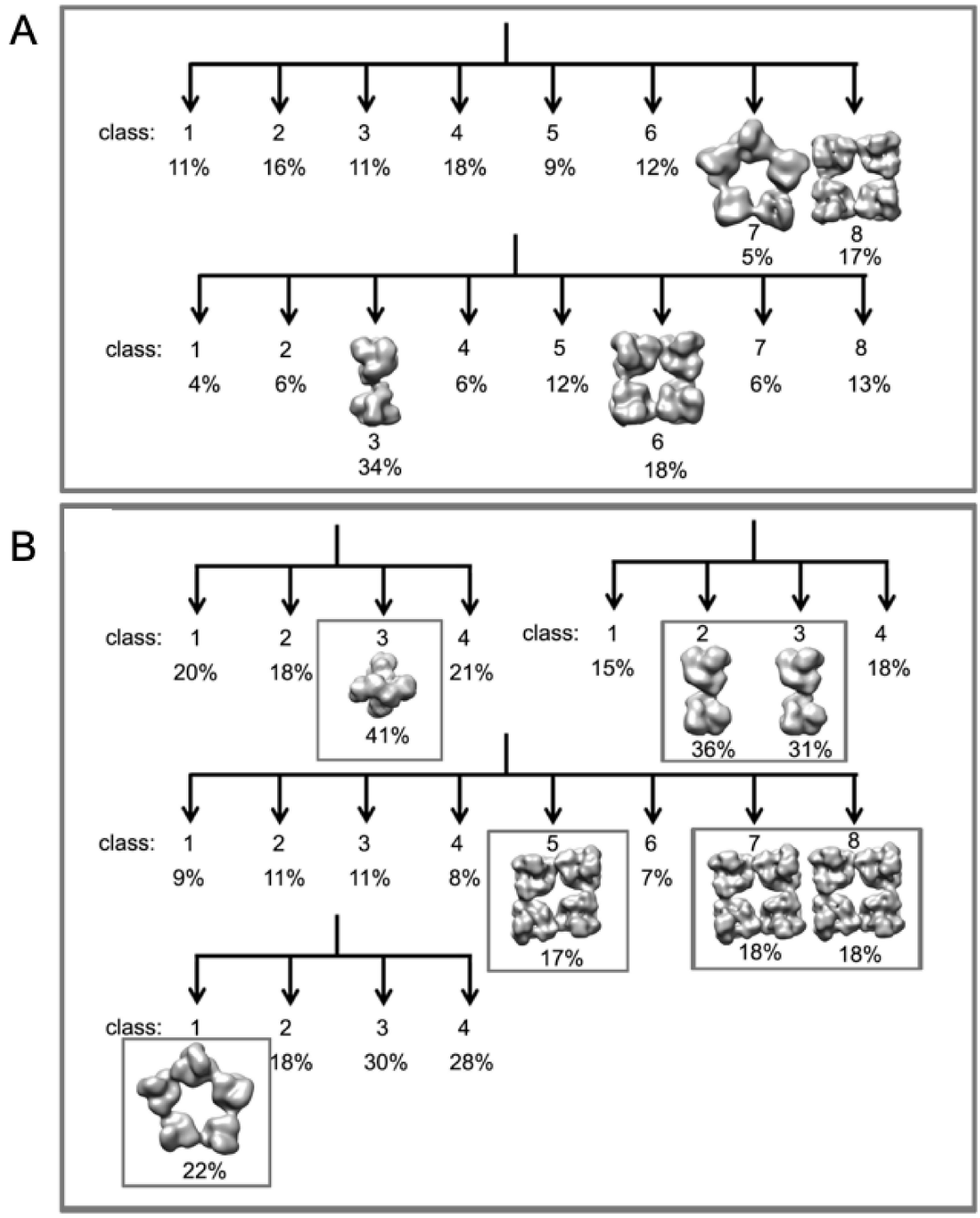

Figure S1 (A) Preliminary 3D classifications performed on the whole GAPDH data set using an ellipsoid (top) and a sphere (bottom) as initial models. (B) 3D classification performed on single GAPDH oligomer data sets. The particles belonging to the boxed 3D classes were used for the final 3D refinement.

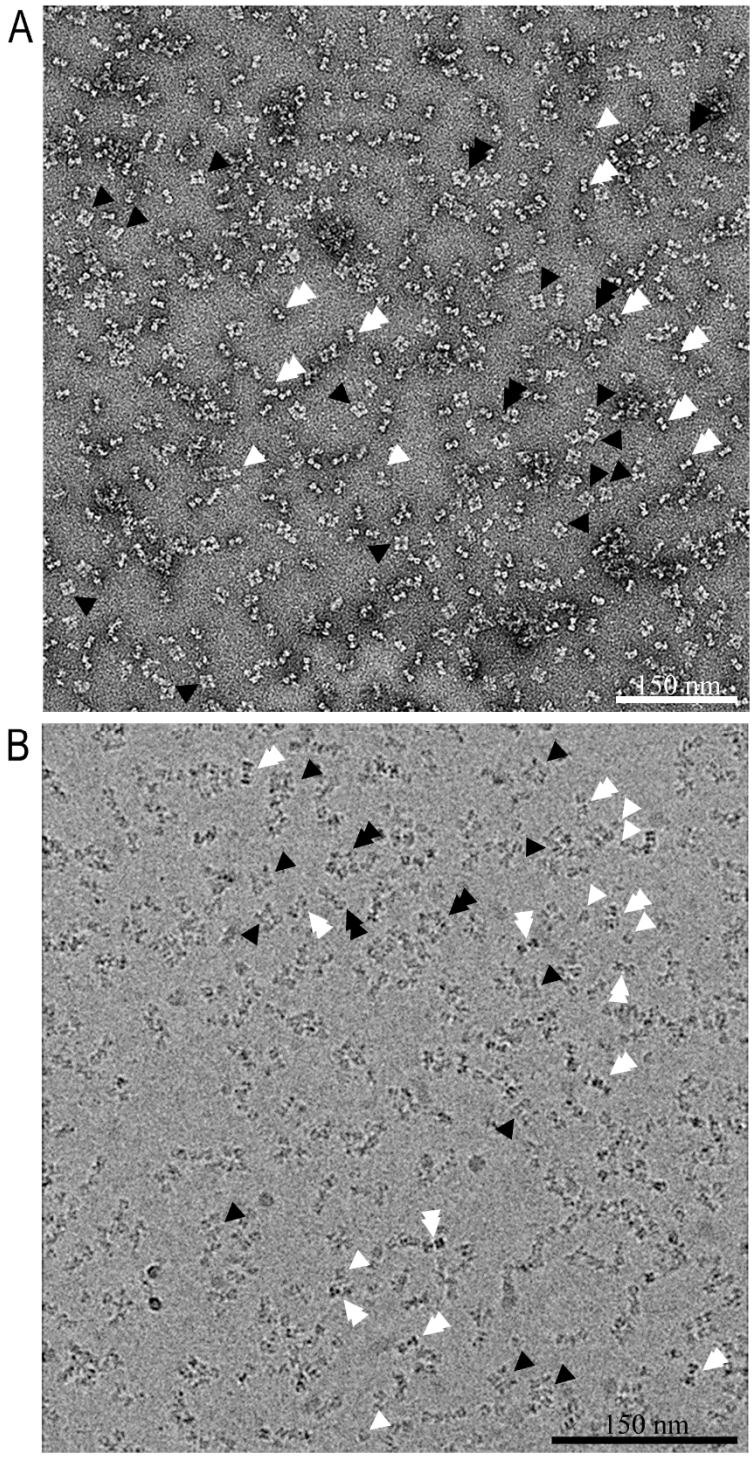

Figure S2 (A) Negative staining and (B) cryoEM representative micrographs. The single and double arrowheads point to the A_2B_2 (single white arrowheads), A_4B_4 (double white arrowheads), A_8B_8 (single black arrowheads) and $A_{10}B_{10}$ (double black arrowheads) projections.

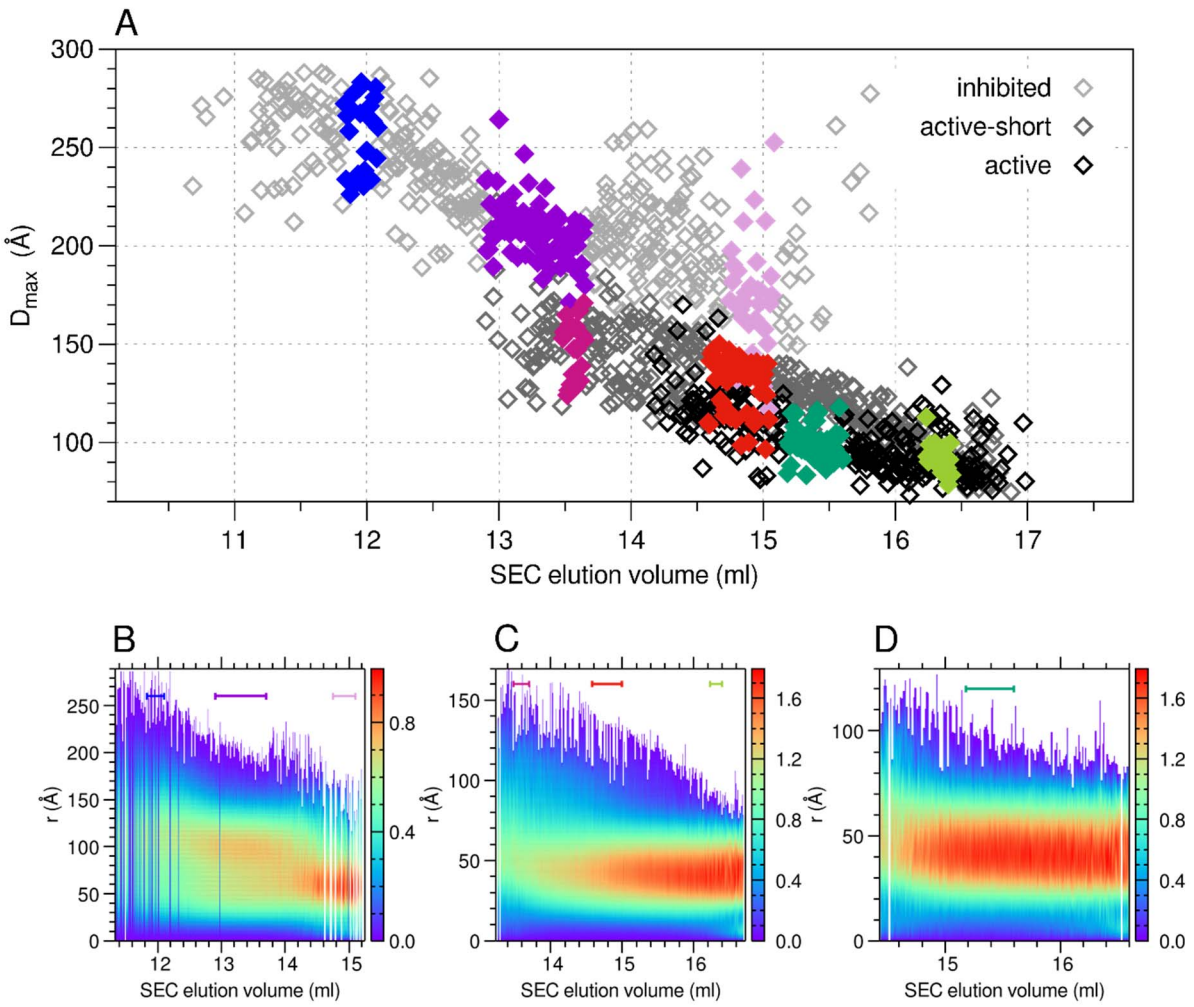

Figure S3 (A) The maximum particle dimension (D_{max}, diamonds) estimated from indirect Fourier transform of the SAXS frames for the three AB-GAPDH samples: inhibited (light grey symbols, maximum at 13 ml), active-short (grey symbols, maximum at 14.8 ml) and active (black symbols, maximum at 15.4 ml), is shown as a function of the SEC elution volume. The data points belonging to the frames averaged to obtain the selected scattering profiles are highlighted with a colour code. 2D maps of (B) inhibited, (C) active-short, (D) active samples analysed by means of SEC-SAXS showing the calculated pair distance distribution function normalized by the subtended area (P(r)/(I(0)), as a function of the SEC elution volume, are presented. The frames averaged to obtain the representative scattering profiles are highlighted by means of bars whose colour key corresponds to that of the plotted P(r) functions in Figure 1.

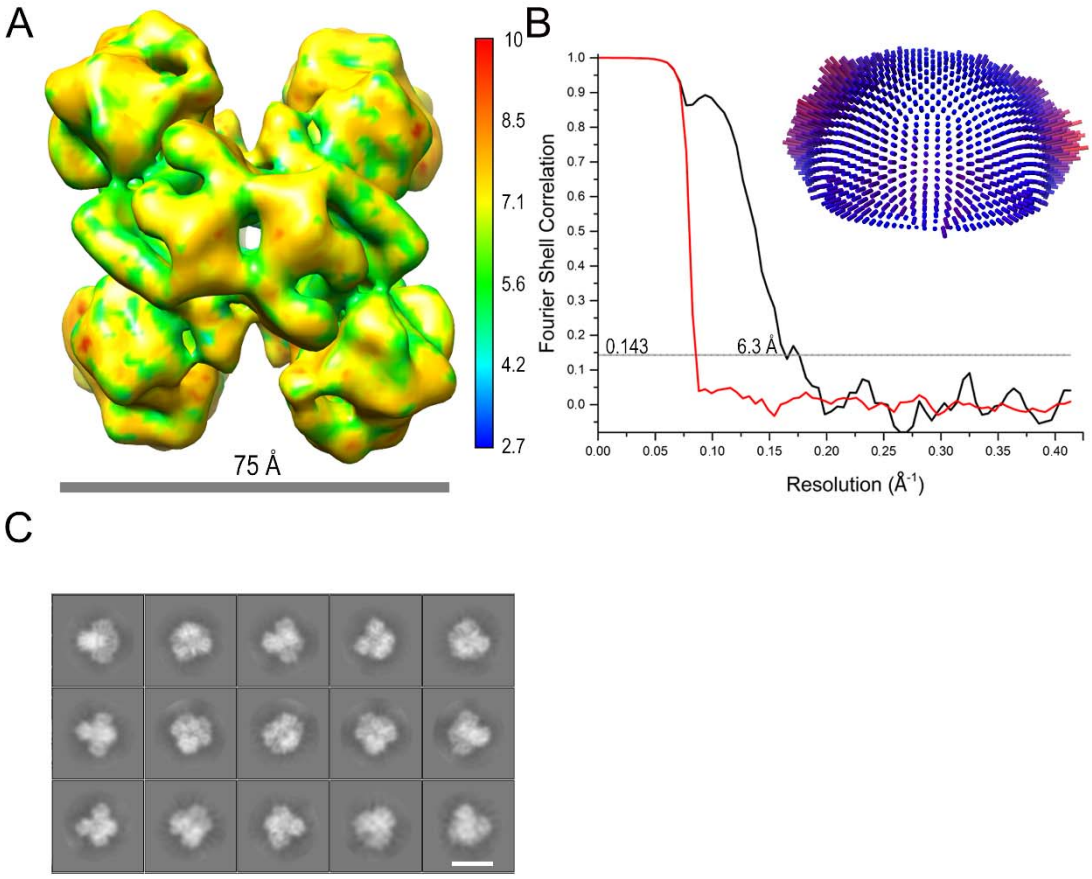

Figure S4 (A) CryoEM electron density map of A_2B_2 oligomer (D2 symmetry) at 6.3 Å resolution filtered according to ResMap local resolution. (B) Fourier shell correlation (FSC) curves (red, FSC phase randomized masked curve; black, FSC corrected curve) of the map with the resolution that corresponds to FSC=0.143 marked. The inset shows the Euler angle distribution. (C) Representative 2D class averages of the A_2B_2 particle images. The scale bar is 80 Å.

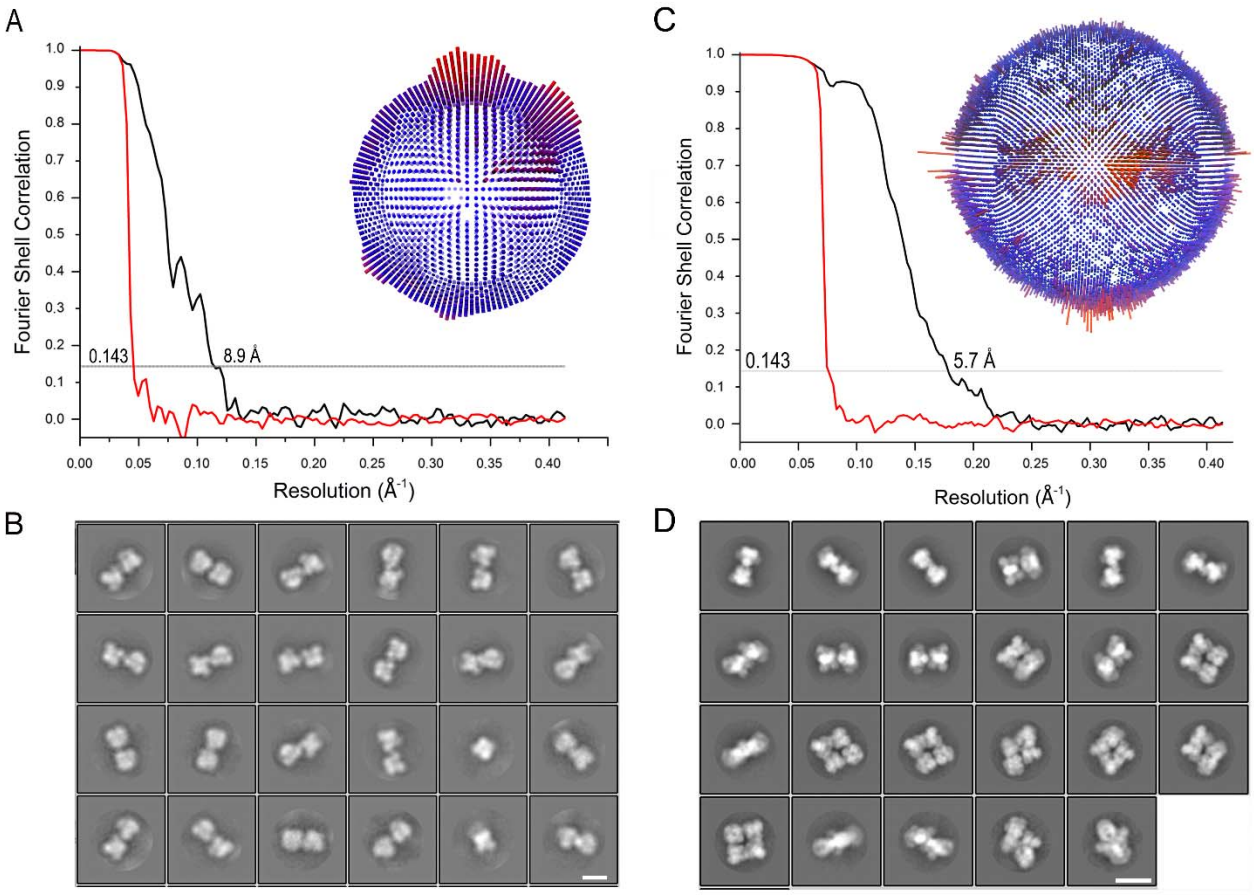

Figure S5 (A) FSC curve of A_4B_4 map (red, FSC phase randomized masked curve; black, FSC corrected curve) with the resolution that corresponds to FSC=0.143 marked. The inset shows the Euler angle distribution. (B) Representative 2D class averages of A_4B_4 particle images. The scale bar is 85Å. (C) FSC curve of the A_8B_8 map (red, FSC phase randomized masked curve; black, FSC corrected curve) with the resolution that corresponds to FSC=0.143 marked. The inset shows the Euler angle distribution. (D) Representative 2D class averages of the A_8B_8 particle images. The scale bar is 150Å.

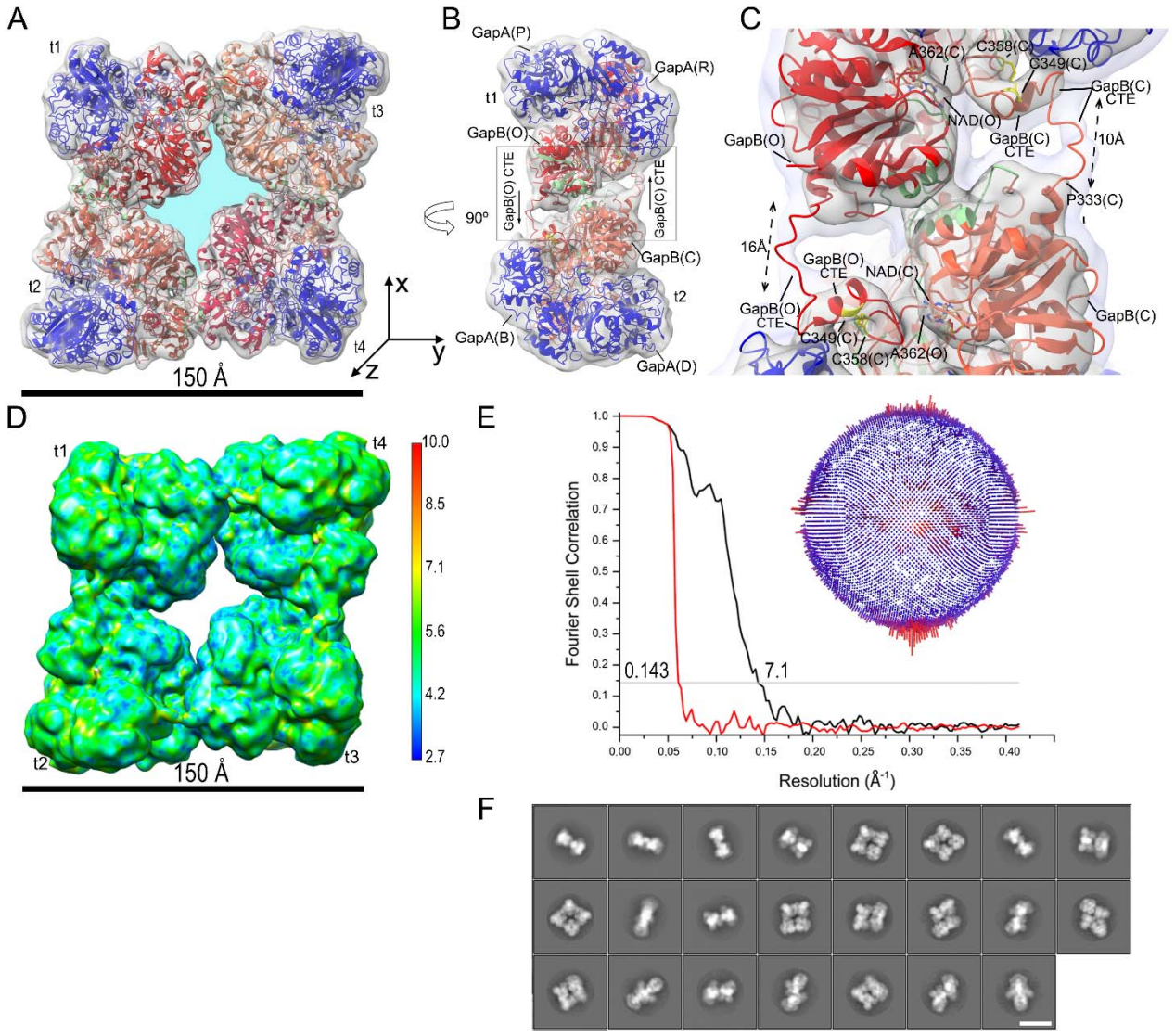

Figure S6 (A) CryoEM electron density map (C2 symmetry) at 7.1 Å fitted with the models derived from the crystal structure of the oxidized A_2B_2 complexed with $NADP^+$ (PDB ID 2PKQ) (Fermani *et al.*, 2007). Labels t1-t4 indicate the A_2B_2 tetramers. The O/Q, A/C, E/G and K/I B-subunits are represented in red, tomato, crimson and coral, respectively. The A-subunits are in blue. The oligomer central cavity (in light blue) has a surface area of 1738 $Å^2$. (B) Side view of the map in (A) shown at low density threshold. (C) Detail of the region boxed in B. The cryoEM electron density map is displayed at two different isosurface levels (high in dark gray and low in light gray). The interfacing residues between adjacent t1 and t2 GAPDH tetramers are highlighted in green. (D) CryoEM electron density map filtered according to ResMap local resolution. (E) FSC curve of the oligomer map (red, FSC phase randomized masked curve; black, FSC corrected curve) with the resolution that corresponds to FSC=0.143 marked. The inset shows the Euler angle distribution. (F) Representative 2D class averages of the A_8B_8 particle images. The scale bar is 150 Å.

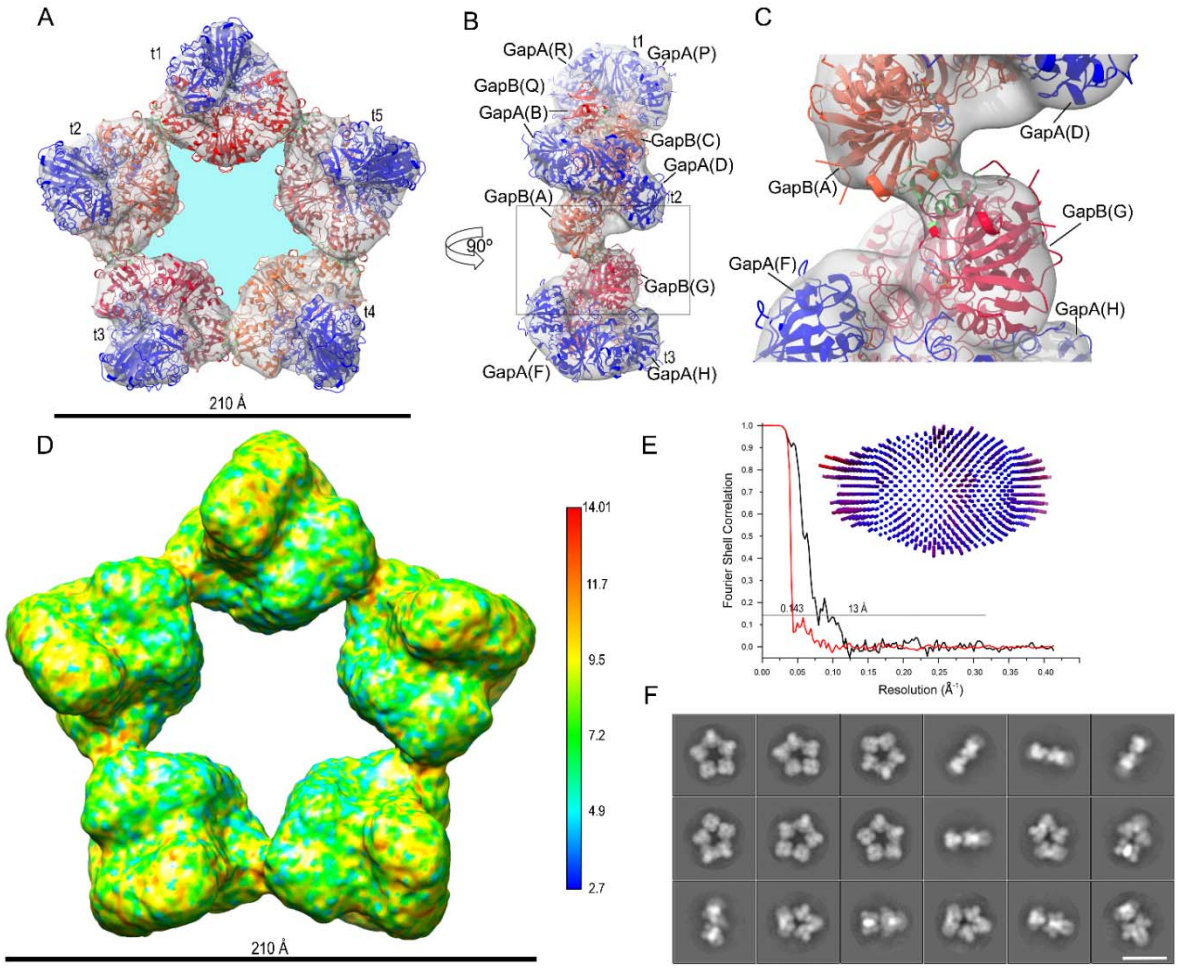

Figure S7 (A) CryoEM electron density map (C5 symmetry) at 13 Å fitted with the models derived from the crystal structure of the oxidized A_2B_2 complexed with NADP+ (PDB ID 2PKQ) (Fermani *et al.*, 2007). Labels t1-t5 indicate the A_2B_2 tetramers. B-subunits are represented in red, tomato, crimson, coral and indian red, while A-subunits are in blue. The oligomer central cavity (in light blue) has a surface area of 5100 $Å^2$. (B) Side view of the map shown in A containing the GAPDH tetramers t1-t3. (C) Detail of the region boxed in B. The interfacing residues between B subunits, i.e. B-subunits (chain A) (tomato) and B-subunits (chain G) (crimson) of adjacent t2 and t3 GAPDH tetramers are highlighted in green. (D) CryoEM electron density map filtered according to ResMap local resolution. (E) FSC curve of the oligomer map (red, FSC phase randomized masked curve; black, FSC corrected curve) with the resolution that corresponds to FSC=0.143 marked. The inset shows the Euler angle distribution. (F) Representative 2D class averages of the $A_{10}B_{10}$ particle images. The scale bar is 200 Å.

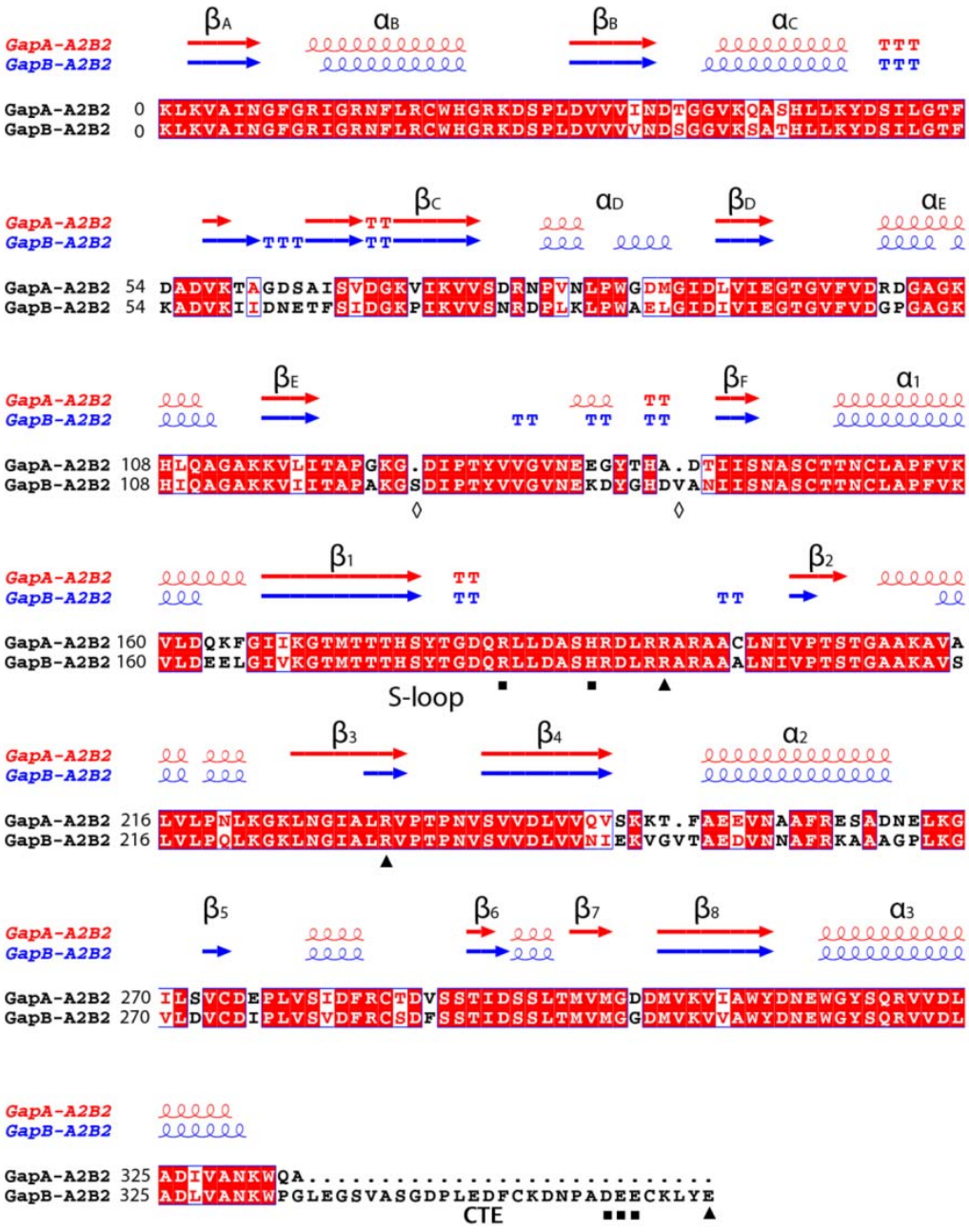

Figure S8 The alignment was performed with ClustalW and visualized with Espript (http://espript.ibcp.fr) using the sequence and the structure of oxidized A_2B_2 B-subunit (chain Q) and A-subunit (chain R) (PDB ID 2PKQ) (Fermani *et al.*, 2007). The black squares and triangles indicate residues likely interacting with CTE residues indicated with the same symbols, of the B subunit belonging to an adjacent tetramer (see main text). White diamonds indicate residue insertions of B-subunit respect to A-subunit.

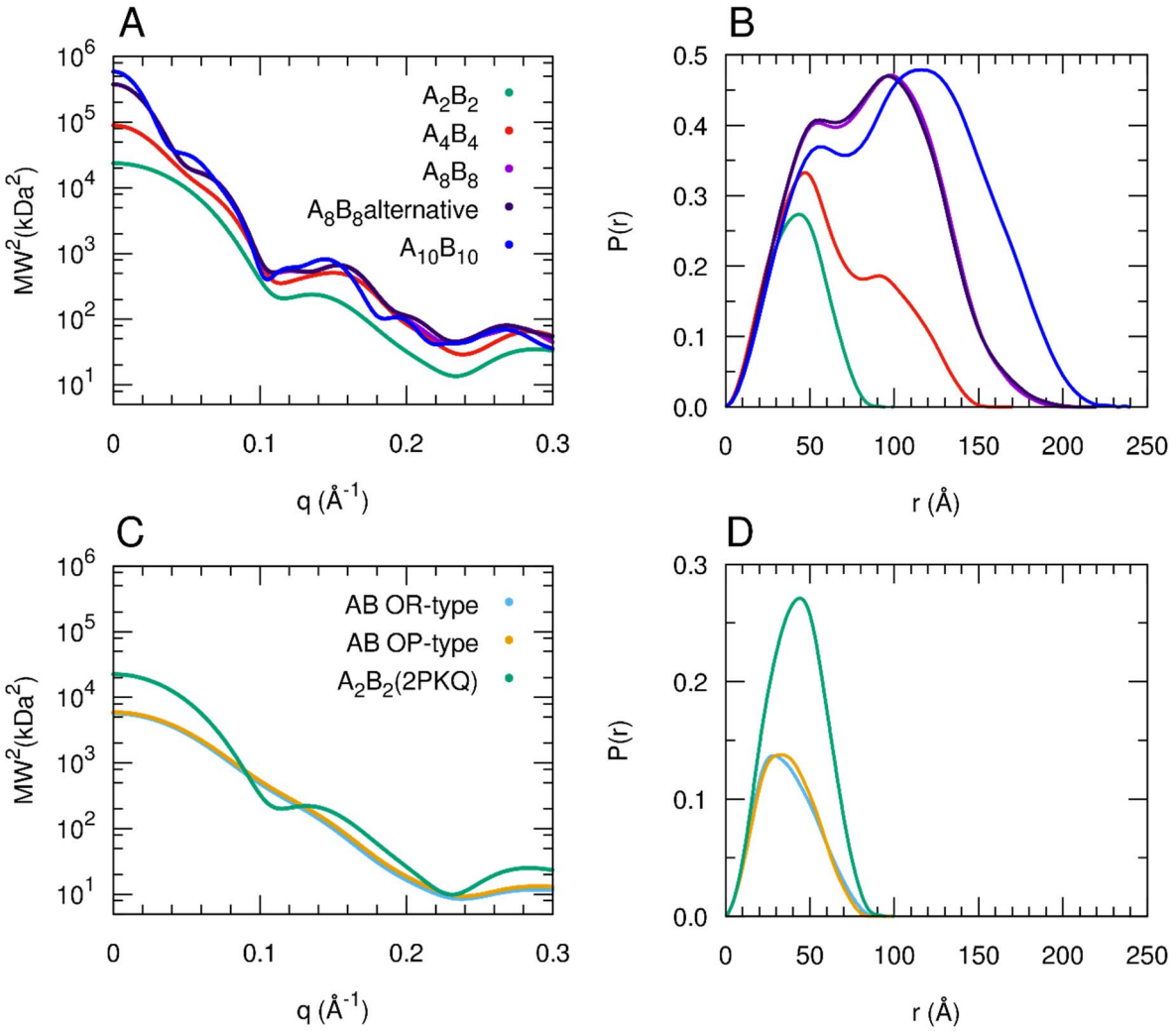

Figure S9 (A) Theoretical scattering profiles calculated from the atomic models of the AB-GAPDH oligomers obtained by cryoEM analysis. In (B) the corresponding pair distance distribution functions (P(r)) provided by indirect Fourier transform of the theoretical profiles are shown. (C) Theoretical scattering profiles calculated from the crystal structure of the AB-GAPDH tetramer in oxidized form complexed with NADP (PDB ID 2PKQ) (Fermani *et al.*, 2007) and from two possible dimeric AB forms. In (D) the corresponding P(r) functions are shown.

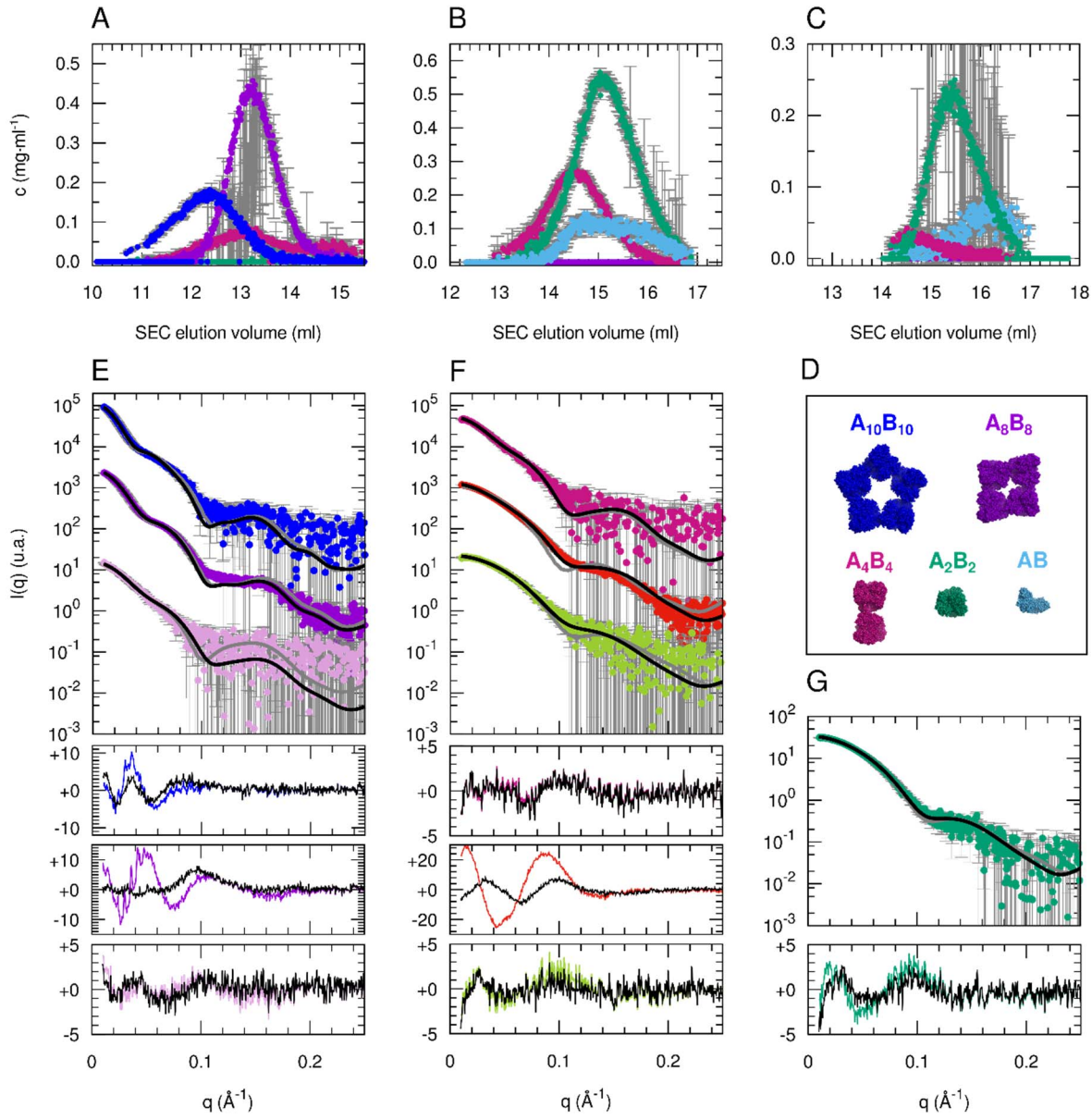

Figure S10 Optimized mass concentrations of the different oligomers as a function of the elution volume (A) for inhibited, (B) for the active-short and (C) for active sample. (D) Color code explanation. (E) Best fit of the three selected average SAXS profiles in the elution of the inhibited sample (blue, violet and pink circles, colour code as in Figure 1A, B) as linear combinations of the AB-GAPDH oligomers $A_{10}B_{10}$, A_8B_8 and A_4B_4 (black lines). The optimized volume fractions are reported in Table S7. The best-fits provided by a single atomic structure ($A_{10}B_{10}$, A_8B_8 and A_4B_4, respectively) are reported as grey lines for comparison. In the panels below error-weighted residual difference plots are reported [$(I_{exp}-I_{calc})/\sigma_{exp}$, where I_{exp} and I_{calc} are the experimental and calculated intensity respectively and σexp are the experimental standard deviations], as black lines for the linear combination fits and as colored lines for the single structure fits. (F) Best fit of the three selected average SAXS profiles in the elution of the active-short sample (purple, red and light green circles, colour code as in Figure 1A, C) as a linear combination of A_4B_4, A_2B_2 or AB (black lines). The best-fits provided by a single atomic

structure (A_4B_4, A_2B_2 and again A_2B_2 respectively) are reported as grey lines for comparison. (G) Best fit of the selected average SAXS profile in the elution of the active sample (green circles, colour code as in Figure 1A, D) as a linear combination of A_4B_4, A_2B_2 or AB (black line). The best-fit provided by a single atomic structure (A_2B_2) is reported as a grey line.

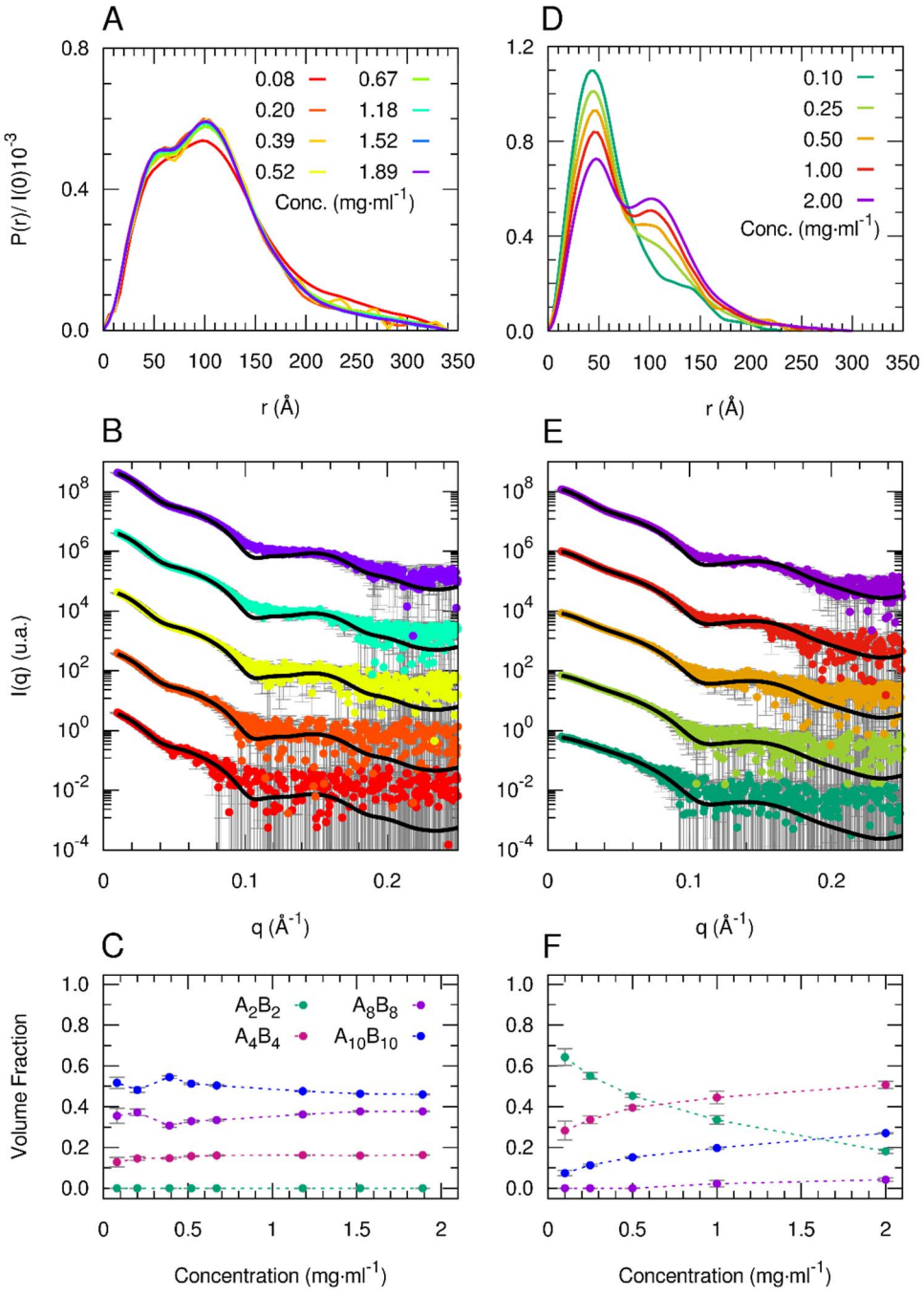

Figure S11 (A) Pair distance distribution functions obtained by indirect Fourier inversion of SAXS data collected on a concentration series of AB-GAPDH incubated in "inhibited" conditions. (B) SAXS profiles of a concentration series of AB-GAPDH incubated in "inhibited" conditions (dots with colour code reported in (A)) and theoretical scattering profiles (black lines) obtained by fitting the data as a linear combination of the form factors calculated from the atomic coordinates of the A_2B_2, A_4B_4, A_8B_8 and $A_{10}B_{10}$ models presented in the manuscript. (C) Volume fractions of the different AB-GAPDH oligomers as a function of protein concentration, obtained from the fitting of SAXS data reported in (B). In panels (D), (E) and (F) the results of the same SAXS data analysis of AB-GAPDH incubated in "active" conditions are reported.

References

Afonine, P.V., Poon, B.K., Read, R.J., Sobolev, O.V., Terwilliger, T.C., Urzhumtsev, A. & Adams, P.D. (2018). Acta Crystallogr. D Struct. Biol. **74**, 531-544.

Fermani, S., Sparla, F., Falini, G., Martelli, P.L., Casadio, R., Pupillo, P., Ripamonti, A. & Trost P. (2007). Proc. Natl. Acad. Sci. U S A **104**, 11109-11114.

Fischer, H., de Oliveira Neto, M., Napolitano, H. B., Polikarpov, I. & Craievich, A. F. (2010). J. Appl. Cryst. **43**, 101-109.

Franke, D., Petoukhov, M. V., Konarev, P. V., Panjkovich, A., Tuukkanen, A., Mertens, H. D. T., Kikhney, A. G., Hajizadeh, N. R., Franklin, J. M., Jeffries, C. M. & Svergun, D. I. (2017). J. Appl. Cryst. **50**, 1212-1225.

Hajizadeh, N.R., Franke, D., Jeffries, C.M. & Svergun, D. I. (2018). Sci. Rep. **8**, 7204.

Krissinel, E. & Henrick, K. (2007). J. Mol. Biol. **372**, 774-797.

Pernot, P., Round, A., Barrett, R., De Maria Antolinos, A., Gobbo, A., Gordon, E., Huet, J., Kieffer, J., Lentini, M., Mattenet, M., Morawe, C., Mueller-Dieckmann, C., Ohlsson, S., Schmid, W., Surr, J., Theveneau, P., Zerrad, L. & McSweeney, S. (2013). J. Synchrotron Rad. **20**, 660-664.

Petoukhov, M. V., Franke, D., Shkumatov, A. V., Tria, G., Kikhney, A. G., Gajda, M., Gorba, C., Mertens, H. D. T., Konarev, P. V. & Svergun, D. I. (2012). J. Appl. Cryst. **45**, 342–350.

Rambo, R. P. & Tainer, J. A. (2013). Nature. **496**, 477–481.